# Mathematical modeling of the graft reaction between polystyrene and polyethylene

Ioana A. Gianoglio Pantano, Adriana Brandolin, Claudia Sarmoria*

*Planta Piloto de Ingeniería Química, PLAPIQUI (UNS-CONICET), Camino La Carrindanga km 7, 8000 Bahía Blanca, Argentina*

## ARTICLE INFO

## ABSTRACT

Polystyrene (PS) and polyethylene (PE) are two major components of household plastic waste whose blends are immiscible. Recycling them together is an attractive option that requires a compatibilization process to improve the blend mechanical properties. If a PE/PS copolymer is added or formed *in situ*, it may act as compatibilizer. The structure and molecular properties of this copolymer are key factors to assure its effectivity as a compatibilizer. In this work, we study the graft copolymerization reaction between polystyrene and polyethylene using the catalytic system composed of AlCl$_3$ and styrene. We develop a model of this process which considers that PE/PS grafting and PS degradation occur simultaneously. We propose a kinetic mechanism for the whole process and apply the method of moments to solve the mass balance equations. The model is able to calculate average molecular weights as well as the amount of grafted PS. It accurately describes the available experimental data, constituting a valuable tool for simulation and optimization purposes.

© 2011 Elsevier Ltd. All rights reserved.

## 1. Introduction

Even though polymer recycling is an attractive tool in current efforts to reduce plastic waste accumulation, when applied to household waste streams it must overcome the challenge of processing immiscible mixtures of different polymers. One example of such immiscible mixtures is given by polystyrene (PS) and the polyolefins (PO), which are two of the majority components of urban polymeric waste. Straightforward blends of these materials show poor mechanical properties. One way of overcoming the problem and obtaining recyclable material is separating the different resins present in the waste stream. In order to avoid the cost associated with such a process, researchers have sought practical methods for dealing with mixtures of polymers. These methods usually involve incorporating a compatibilizer to the mixture or generating one *in situ* through the addition of a suitable reagent [1,2]. This compatibilizer reduces the droplet coalescence and increases the interfacial strength, thus improving the mechanical properties of the blend [3,4].

When the PO involved in the blends is polyethylene (PE), one of the possible compatibilizers is a PE-g-PS graft copolymer. It is possible to produce such a copolymer from a mixture of PS and PE through a Friedel-Crafts alkylation [5–10]. This requires adding a strong Lewis acid as catalyst. A cocatalyst such as styrene may also be added to improve the yield of the reaction [6–8].

Carrick [5] studied the reaction of PS and PE with AlCl$_3$ in a cyclohexane solution and reported the formation of PE-g-PS graft copolymer. The amount of grafted PS exhibits a maximum, suggesting that the initially formed copolymer undergoes subsequent degradation. Under similar reaction conditions he studied the degradation of PE and reported the occurrence of isomerization in addition to the degradation reaction.

Sun and Baker [6] studied the PE/PS compatibilization using a Friedel-Crafts alkylation in the molten state. They tested different Lewis acids and found that a cocatalyst, such as a cationically polymerizable monomer or a halogenated alkane, increased the amount of grafted PS. Their results showed that the most efficient catalytic system was AlCl$_3$ with styrene.

Díaz et al. [7,8] analyzed the reaction of PS and PE with AlCl$_3$ and styrene as catalytic system. They investigated the effect of PE chain length on the yield of copolymer, the interfacial adhesion and the mechanical properties of the resulting mixture. Shorter PE chains appeared to be more reactive, suggesting that their higher mobility allowed them to reach more readily the interface where the grafting reaction takes place. The authors also evaluated the effect of the catalytic system in detail, varying the concentrations of AlCl$_3$ and styrene in a wide range. They found that at their operating conditions PE was not involved in any secondary reactions, but PS

* Corresponding author. Tel.: +54 291 4861700; fax: +54 291 4861600.
  *E-mail address:* csarmoria@plapiqui.edu.ar (C. Sarmoria).

suffered both chain scission and chain combination [7,11,12]. According to their data, PS chain scission increased with AlCl$_3$ concentration and was curbed by the presence of styrene. Based on this experimental evidence, in a previous work [13] we modeled the degradation of PS in the presence of AlCl$_3$ only. The proposed model considered that the reaction of PS with AlCl$_3$ leads initially to the elimination of a PS phenyl group, generating a benzene molecule and a polymeric carbonium ion. Afterward, the carbonium ion may induce either PS chain scission or the formation of an indane skeleton in the PS chain, in agreement with the findings of Nanbu et al. [14]. Our previous model considered that PS chain scission is produced by the cleavage of weak and normal PS bonds, in accordance with the experimental evidence of Chiantore et al. [15]. The initial fast degradation is due to the breakage of weak bonds, while molecular weight reduction at large reaction times results from the scission of normal bonds. The latter may only occur when high catalyst concentrations are used.

The analysis of the side reactions involving PS and PE is important in order to be able to propose a complete kinetic mechanism, since they may affect the properties of the final graft copolymer. Although some mechanisms have been proposed in the literature [5] the reaction process is not yet completely understood. For this reason, the reactivities of PS and PE in the presence of the AlCl$_3$/styrene catalytic system must be analyzed in order to obtain consistent information prior to proposing a complete kinetic mechanism for the Friedel-Crafts graft reaction.

Rabek and Lucki [16] reported the formation of a complex between PS and AlCl$_3$ as well as the crosslinking of PS when a solvent is added. Theoretical investigation of benzene–AlCl$_3$ and ethylene–AlCl$_3$ interactions suggests that Lewis acids have a significant role in the aromatic ring activation in reactions involving electrophilic aromatic substitution. It also plays an important role in the olefinic activation in addition reactions [17]. Several works have reported the presence of unsaturations in the PE chain, apparently produced during PE processing [18,19]. Similarly, PE thermal and thermo-catalytic degradations are reported to produce double bonds, the isomerization of which is enhanced by catalyst acidity [20,21]. All the reported evidence suggests that PS and PE are reactive enough to form a PE-g-PS copolymer in the presence of AlCl$_3$.

In the present work we focus on modeling the complete grafting reaction. Our model considers not only the PE-g-PS graft copolymerization reactions in the presence of AlCl$_3$ and styrene, but also the side reactions that PS suffers at the copolymerization conditions. The model is an extension of the previous one that describes the reaction between PS and AlCl$_3$ only [13]. For the copolymerization model we propose a kinetic mechanism from which we derive the mass balance equations for all the reactive species. These equations are simplified using the method of moments. Experimental data obtained in our laboratory [7,11,12] are used to estimate the model kinetic parameters. The resulting model describes appropriately the evolution with time of the measured variables, such as average molecular weights and mass percentage of grafted PS.

## 2. Mathematical model

### 2.1. Kinetic mechanism

The catalyst AlCl$_3$ may activate aromatic rings present both in PS and styrene, as well as unsaturations present in PE. Once activation of the appropriate groups has occurred, the PE-g-PS copolymer may be formed. In other words, the activated PE may react with styrene, and subsequently with PS to form the copolymer, or, in the absence of styrene, activated PE may react with benzene produced during PS scission, and then with PS to form the copolymer. Similarly, PS may react with styrene leading to chain scission and chain combination reactions as reported elsewhere [12]. Reactions in this system have been reported to proceed by a cationic mechanism. The absence of free radical reactions was confirmed experimentally [12].

In order to obtain a simple model, the Friedel-Crafts alkylation is considered to occur in a single step involving PS, PE, AlCl$_3$ and either styrene or benzene. Benzene is not added to the reactive mixture but produced by the reaction of PS with AlCl$_3$, as explained later. Once reacted, the molecules of styrene or benzene are assumed to become part of the synthesized copolymer, where they are considered as styrene monomeric units.

Since the PS and PE homopolymers form two immiscible phases, the grafting reaction should take place at the polymer–polymer interface. For this reason, equations describing the diffusion process should have been taken into account together with mass balances. The complete system of equations should reflect the experimentally observed fact that smaller molecules reach the interface more readily and are more reactive than the larger ones [3,7,23,24]. As a first approximation, we have assumed that the grafting reaction takes place in a single phase to which smaller molecules have preferential access.

The secondary reactions for the PS chains are those previously proposed for the effect of AlCl$_3$ alone [13], plus those associated to the effect of the complete catalytic system, AlCl$_3$/styrene. When adding only AlCl$_3$ to molten PS, the reactions proposed in the previous model [13] included: chain scission, produced by the cleavage of weak and normal bonds present in the PS chain, formation of an indane group in the chain backbone, chain combination and decomposition of the catalyst. In this work, we propose that the treatment of PS with AlCl$_3$ and styrene involves all the reactions just mentioned, plus the following reactions where styrene or both AlCl$_3$ and styrene participate: PS random chain scission of both weak and normal bonds, chain combination by addition of a styrene molecule, styrene polymerization on PS chains and the deactivation of AlCl$_3$ and styrene by a reaction between them. The presence of a deactivation reaction between styrene and AlCl$_3$ was suggested by the experimental observation [25] that when mixing the catalyst and cocatalyst prior to their addition to a molten mixture of PS and PE the copolymer yield was poorer than when the catalyst and cocatalyst were added separately to the melt. Since experimental evidence [7] indicates that PE does not degrade under the reaction conditions used, no side reactions for PE are proposed. In the resulting simplified mechanism we consider the equations summarized in Table 1. The kinetic equations are shown together with the corresponding reaction rates. The latter are indicated as $R_i$, where $i$ is the equation number.

In Equations (1)–(12), PS($x$) is a polystyrene molecule with $x$ monomeric units, PE($x$) is a polyethylene molecule with $x$ monomeric units, $G(x,y)$ is a PE-g-PS copolymer molecule with $x$ styrene monomeric units and $y$ ethylene monomeric units, $S$ is a styrene molecule, $A$ is an active catalyst molecule, $Ai$ and $Si$ are catalyst and cocatalyst molecules that are inactive toward the Friedel-Crafts reaction, and $B$ is a benzene molecule.

Since we assume that the polymerization of styrene on PS chains could only occur on the chain ends, each PS($x$) molecule has two sites available for that reaction. For the remaining reactions that involve PS, any of the monomeric units along the chain may participate. That is why each PS($x$) has $x$ sites available to all reactions except polymerization of styrene. Under the conditions used for this treatment PE may only participate in the grafting reaction, and since it may only be grafted through its ends, each PE molecule is assumed to have two active sites. Reactions are 1st order with respect to the reactive sites. The reaction orders with

**Table 1**
Kinetic model.

| Kinetic equation | $R_i$ |
|---|---|
| **Graft reactions** | |
| $PS(x) + PE(y) + A + B \xrightarrow{k_{gB}} G(x+1,y) + A \quad x = 1, ..., \infty; \quad y = 1, ..., \infty$ (1) | $R_1(x,y) = 2f_r k_{gB} A\, B\, x\, PS(x)PE(y)$ |
| $PS(x) + PE(y) + A + S \xrightarrow{k_{gS}} G(x+1,y) + A \quad x = 1, ..., \infty; \quad y = 1, ..., \infty$ (2) | $R_2(x,y) = 2f_r k_{gS} A\, S\, x\, PS(x)PE(y)$ |
| **PS side reactions** | |
| Chain scission through weak links I) | |
| $PS(x) + A \xrightarrow{k_{S1w}} PS(x-y-1) + PS(y) + A + B \quad x = 2, ..., \infty$ (3) | $R_3(x) = k_{S1w} f_w A^2 x\, PS(x)$ |
| Chain scission through weak links II) | |
| $PS(x) + A + S \xrightarrow{k_{S2w}} PS(x-y-1) + PS(y) + A + B + S \quad x = 2, ..., \infty$ (4) | $R_4(x) = k_{S2w} f_w A^{\phi} S^{\kappa} x\, PS(x)$ |
| Chain scission through normal links I) | |
| $PS(x) + A \xrightarrow{k_{S1n}} PS(x-y-1) + PS(y) + A + B \quad x = 2, ..., \infty$ (5) | $R_5(x) = k_{S1n} f_n A^4 x\, PS(x)$ |
| Chain scission through normal links II) | |
| $PS(x) + A + S \xrightarrow{k_{S2n}} PS(x-y-1) + PS(y) + A + B + S \quad x = 2, ..., \infty$ (6) | $R_6(x) = k_{S2n} f_n A^{\eta} S^{\lambda} x\, PS(x)$ |
| Formation of indane skeleton | |
| $PS(x) + A \xrightarrow{k_{In}} PS(x-1) + A + B \quad x = 2, ..., \infty$ (7) | $R_7(x) = k_{In} A^2 x\, PS(x)$ |
| Chain combination I) | |
| $PS(x) + PS(y) + A \xrightarrow{k_{c1}} PS(x+y) + A \quad x = 2, ..., \infty$ (8) | $R_8(x,y) = k_{c1} A^2 x\, PS(x) y\, PS(y)$ |
| Chain combination II) | |
| $PS(x) + PS(y) + A + S \xrightarrow{k_{c2}} PS(x+y) + A + S \quad x = 2, ..., \infty$ (9) | $R_9(x,y) = (k_{c2,1} A^{\xi} S^{\psi} + k_{c2,2} A^{\rho} S^{\upsilon}) x\, PS(x) y\, PS(y)$ |
| Styrene polymerization | |
| $PS(x) + A + S \xrightarrow{k_p} PS(x+1) + A \quad x = 1, ..., \infty$ (10) | $R_{10}(x) = 2 k_p A^{\omega} S^{\tau} PS(x)$ |
| **Catalytic system deactivation** | |
| Catalyst decomposition | |
| $A \xrightarrow{k_i} Ai$ (11) | $R_{11} = k_i A$ |
| Catalyst-styrene reaction | |
| $A + S \xrightarrow{k_d} Ai + Si$ (12) | $R_{12} = k_d A^{\sigma} S^{\chi}$ |

respect to the catalyst and cocatalyst concentrations were used as adjustable parameters according to the expressions shown in the second column of Table 1. Four of the side reactions were part of the kinetic mechanism of the degradation of PS in the presence of AlCl₃ presented in a previous work [13]. They are Equations (3), (5), (7) and (8). For those four reactions we used the same reaction orders with respect to catalyst and cocatalyst concentrations reported previously. The constant $k_{c2}$ in Equation (9) is defined as the sum of two terms as: $k_{c2} = k_{c2,1} A^{\xi} S^{\psi} + k_{c2,2} A^{\rho} S^{\upsilon}$. This definition makes the model more sensitive to the differences observed in the experimental behavior of the system for different $S/A$ ratios.

In the rate expressions corresponding to Equations (1) and (2), $f_r$ is a reactivity factor that takes into account that shorter polymer molecules are more reactive for the grafting reaction than the longer ones, as reported elsewhere [3,7,23,24]. The expression we adopted for this factor, $f_r = 1/M_n P_n$, was the simplest one that would permit shorter molecules to have preferential access to the grafting reaction. In the latter expression, $M_n$ and $P_n$ are the number average molecular weights of PS and PE, respectively.

The process is modeled as being carried out in a constant volume, perfectly stirred batch reactor at isothermal conditions. The mass balances for the species that take part of the reactions described in Equations (1)–(12) are presented in Equations (13)–(18). Brackets are omitted when expressing species molar concentrations.

## 2.2. Mass balances

PS molecules with x monomeric units ($x = 1, ..., \infty$)

$$\frac{dPS(x)}{dt} = -\sum_{i=3}^{6} R_i(x)(1-\delta_{x,1}) + 2\sum_{y=x+1}^{\infty} \Omega(x,y) \sum_{i=3}^{6} R_i(y)$$
$$- R_7(x)(1-\delta_{x,1}) + R_7(x+1) - R_{10}(x) + R_{10}(x-1)$$
$$- \sum_{y=1}^{\infty}(R_8(x,y) + R_9(x,y)) + \frac{1}{2}\sum_{y=1}^{x-1}(R_8(x-y,y)$$
$$+ R_9(x-y,y))(1-\delta_{x,1}) - \sum_{y=1}^{\infty}(R_1(x,y) + R_2(x,y)) \quad (13)$$

PE molecules with x monomeric units ($x = 1, ..., \infty$)

$$\frac{dPE(x)}{dt} = -\sum_{y=1}^{\infty}(R_1(y,x) + R_2(y,x)) \quad (14)$$

PE-g-PS graft copolymer molecules with x styrene monomeric units and y ethylene monomeric units ($x = 2, ..., \infty$, $y = 1, ..., \infty$)

$$\frac{dG(x,y)}{dt} = R_1(x-1,y) + R_2(x-1,y) \tag{15}$$

*Benzene*

$$\frac{dB}{dt} = \sum_{x=2}^{\infty}\sum_{i=3}^{7} R_i(x) - \sum_{x=1}^{\infty}\sum_{y=1}^{\infty} R_1(x,y) \tag{16}$$

*Styrene*

$$\frac{dS}{dt} = -\sum_{x=1}^{\infty} R_{10}(x) - R_{12} - \sum_{x=1}^{\infty}\sum_{y=1}^{\infty} R_2(x,y) \tag{17}$$

*Catalyst*

$$\frac{dA}{dt} = -R_{11} - R_{12} \tag{18}$$

In the above equations, $\mathcal{Q}(x, y)$ determines the distribution of scission products and is given by $1/y$ for random scission [22]. The difference in molar mass between benzene and styrene is neglected. The symbol $f_w$ represents the fraction of weak bonds, and $f_n$ represents the fraction of normal bonds, both defined as in our previous work [13] as

$$f_w = \frac{e_w}{e_n + e_w} = \frac{e_w}{\sum_{x=1}^{\infty}(x-1)P(x)} = \frac{e_w}{\sum_{x=1}^{\infty}xP(x) - \sum_{x=1}^{\infty}P(x)}$$
$$= 1 - f_n \tag{19}$$

where $e_w$ is the concentration of weak bonds and $e_n$ is the concentration of normal bonds. Their initial concentrations were estimated by fitting a model for the degradation of PS in the presence of AlCl$_3$ alone to experimental data [13].

The time evolution of the concentration of PS weak bonds ($e_w$) can be expressed as

$$\frac{de_w}{dt} = -e_w\left(k_{S1w}A^2 + k_{S2w}A^{\phi}S^{\kappa}\right) \tag{20}$$

Equations (19) and (20) must be solved together with the mass balances of the species (Equations (13)–(18)).

Since the number of monomer units in homopolymer and copolymer molecules may range between one and infinity, there are infinitely many mass balance equations. In order to reduce the system size, the well-known method of moments is used to calculate average properties. For that purpose, moment definitions are applied to polymer distributions.

The $a$th order moments for PS and PE mass distributions are defined, respectively, by

$$M_a = \sum_{x=1}^{\infty} (M_S x)^a \mathrm{PS}(x) \tag{21}$$

$$P_a = \sum_{x=1}^{\infty} (M_E x)^a \mathrm{PE}(x) \tag{22}$$

In the above equation, $M_S$ and $M_E$ are the PS and PE monomer molecular weights, respectively.

Double moments are defined similarly. For example, the $a$th, $b$th order moment for the PE-g-PS graft copolymer mass distribution is defined by

$$I_{a,b} = \sum_{x=2}^{\infty}\sum_{y=1}^{\infty} (M_S x)^a (M_E y)^b G(x,y) \tag{23}$$

Experimental data consist in number and weight average molecular weights, and the amount of grafted PS. These quantities may be calculated in terms of several moments of the mass distributions of PS, PE and PE-g-PS as indicated in Table 2.

Table 2 also shows the expressions for calculated number and weight average molecular weights for the graft copolymer. Despite the absence of experimentally measured values against which model predictions could be compared, the latter are valuable for the insight they provide.

In order to transform the mass balances to include moments, all terms in Equations (13) and (14) are multiplied by $(M_S x)^a$ and $(M_E y)^a$, respectively. Each resulting equation then is added up for all polymer lengths. In the same way, all terms in Equation (15) are multiplied by $(M_S x)^a (M_E y)^b$ and then the resulting equation is added up for all block lengths, namely $x$ and $y$. Equations (16), (17) and (20) can also be rearranged as functions of the zeroth and 1st order moments. After rearranging terms, the following equations result:

### 2.3. Moments balances

*Benzene*

$$\frac{dB}{dt} = \left[f_w\left(k_{S1w}A^2 + k_{S2w}A^{\phi}S^{\kappa}\right) + f_n\left(k_{S1n}A^4 + k_{S2n}A^{\eta}S^{\lambda}\right)\right.$$
$$\left. + k_{In}A^2\right]\frac{M_1}{M_S} - 2k_{gB}ABf_r\frac{M_1 P_0}{M_S} \tag{24}$$

*Styrene*

$$\frac{dS}{dt} = -2k_p A^{\omega}S^{\tau}M_0 - R_{12} - 2k_{gS}ASf_r\frac{M_1 P_0}{M_S} \tag{25}$$

*0th order homopolymer moments*

$$\frac{dM_0}{dt} = \left[f_w\left(k_{S1w}A^2 + k_{S2w}A^{\phi}S^{\kappa}\right) + f_n\left(k_{S1n}A^4 + k_{S2n}A^{\eta}S^{\lambda}\right)\right]$$
$$\left(\frac{M_1}{M_S} - 2M_0\right) - \frac{1}{2}\left(k_{c1}A^2 + k_{c2,1}A^{\xi}S^{\psi} + k_{c2,2}A^{\rho}S^{\upsilon}\right)$$
$$\frac{M_1^2}{M_S} - 2A(k_{gB}B + k_{gS}S)\frac{M_1 P_0}{M_S M_n P_n} \tag{26}$$

$$\frac{dP_0}{dt} = -2A(k_{gB}B + k_{gS}S)\frac{M_1 P_0}{M_S M_n P_n} \tag{27}$$

*1st order homopolymer moments*

$$\frac{dM_1}{dt} = -\left[f_w\left(k_{S1w}A^2 + k_{S2w}A^{\phi}S^{\kappa}\right) + f_n\left(k_{S1n}A^4 + k_{S2n}A^{\eta}S^{\lambda}\right)\right]M_1$$
$$- k_{In}A^2 M_1 + 2M_S k_p A^{\omega}S^{\tau}M_0 - 2A(k_{gS}S + k_{gB}B)\frac{M_2 P_0}{M_S M_n P_n} \tag{28}$$

**Table 2**
Molecular weights and mass of grafted PS in terms of moments.

|  | PS | PE | PE-g-PS |
|---|---|---|---|
| Number average molecular weight | $M_n = \frac{M_1}{M_0}$ | $P_n = \frac{P_1}{P_0}$ | $I_n = \frac{I_{1,0} + I_{0,1}}{I_{0,0}}$ |
| Weight average molecular weight | $M_w = \frac{M_2}{M_1}$ | $P_w = \frac{P_2}{P_1}$ | $I_w = \frac{I_{2,0} + 2I_{1,1} + I_{0,2}}{I_{1,0} + I_{0,1}}$ |
| % wt of grafted PS | $Gr = 100\frac{I_{1,0}}{M_{1(t=0)}}$ |  |  |

$$\frac{dP_1}{dt} = -2A(k_{gB}B + k_{gS}S)\frac{M_1 P_1}{M_S M_n P_n} \tag{29}$$

*2nd order homopolymer moments*

$$\frac{dM_2}{dt} = \left[f_w\left(k_{S1w}A^2 + k_{S2w}A^\phi S^\kappa\right) + f_n\left(k_{S1n}A^4 + k_{S2n}A^\eta S^\lambda\right)\right]$$
$$\left(-\frac{M_3}{3M_S} - M_2 + \frac{M_S M_1}{3}\right) + k_{In}A^2(-2M_2 + M_S M_1)$$
$$+ \left(k_{c1}A^2 + k_{c2,1}A^\xi S^\psi + k_{c2,2}A^\rho S^\upsilon\right)\left(\frac{M_2}{M_S}\right)^2 + 2k_p A^\omega S^\tau$$
$$\left(2M_S M_1 + M_s^2 M_0\right) - 2A(Sk_{gS} + Bk_{gB})\frac{M_3 P_0}{M_S M_n P_n} \tag{30}$$

$$\frac{dP_2}{dt} = -2A(k_{gB}B + k_{gS}S)\frac{M_1 P_2}{M_S M_n P_n} \tag{31}$$

*0th−0th order copolymer moment*

$$\frac{dI_{0,0}}{dt} = 2A(k_{gB}B + k_{gS}S)\frac{M_1 P_0}{M_S M_n P_n} \tag{32}$$

*1st−0th order copolymer moment*

$$\frac{dI_{1,0}}{dt} = 2A(k_{gB}B + k_{gS}S)\left(\frac{M_2}{M_S} + M_1\right)\frac{P_0}{M_n P_n} \tag{33}$$

*0th−1st order copolymer moment*

$$\frac{dI_{0,1}}{dt} = 2A(k_{gB}B + k_{gS}S)\frac{M_1 P_1}{M_S M_n P_n} \tag{34}$$

*1st−1st order copolymer moment*

$$\frac{dI_{1,1}}{dt} = 2A(k_{gB}B + k_{gS}S)\left(\frac{M_2}{M_S} + M_1\right)\frac{P_1}{M_n P_n} \tag{35}$$

*2nd−0th order copolymer moment*

$$\frac{dI_{2,0}}{dt} = 2A(k_{gB}B + k_{gS}S)\left(\frac{M_3}{M_S} + 2M_2 + M_s M_1\right)\frac{P_0}{M_n P_n} \tag{36}$$

*0th−2nd order copolymer moment*

$$\frac{dI_{0,2}}{dt} = 2A(k_{gB}B + k_{gS}S)\frac{M_1 P_2}{M_S M_n P_n} \tag{37}$$

*Fraction of weak bonds*

$$f_w = \frac{e_w}{\frac{M_1}{M_S} - M_0} \tag{38}$$

The selected moment definitions correspond to mass distributions, not to length distributions. Since the latter appear in some of the terms in the original mass balances (Equations (13)–(17)), a factor $1/M_S$ is used to make the conversion between mass and length distributions.

One should note that when solving for the 2nd PS moment, the 3rd order moment appears in the equation. Its value was estimated using a closure technique [26], making it possible to obtain expressions of the higher order moments in terms of the known lower order ones. When the type of distribution is not known

**Table 3**
Conditions used for the graft reaction experiments [7,11].

| | | |
|---|---|---|
| Virgin PE | PE62: ($P_w = 52,000$, $P_n = 16,700$) | PE65: ($P_w = 40,000$, $P_n = 11,000$) |
| Virgin PS | PS ($M_w = 271,000$, $M_n = 136,000$) | |
| PS/PE | 20/80 % wt | |
| Reaction time | 10 min | 18 min |
| Initial styrene concentration | 0.3 % wt | |
| Initial AlCl$_3$ concentration | 0.1 % wt | 0.3 % wt |
| | 0.3 % wt | 1 % wt |
| | 0.5 % wt | |
| | 0.7 % wt | |
| | 1 % wt | |
| | 1.5 % wt | |
| Reaction conditions | Batch mixer at 190 °C under N$_2$ atmosphere | |

beforehand, as is the case in our system, the result is an approximate solution. In this model we use the expression corresponding to a log-normal distribution (Equation (39)).

$$M_3 = M_0\left(\frac{M_2}{M_1}\right)^3 \tag{39}$$

This choice of closure equation does not imply that the calculated distribution will be log-normal. Of course, the closer the actual distribution is to log-normal, the better will be the accuracy of the calculated results. Further details on the closure technique may be found elsewhere [26].

As input data the model requires the mass of the homopolymers, PS and PE, together with their initial number and weight average molecular weights, mass of catalyst and cocatalyst, operating temperature and residence time. Parameter values, such as kinetic rate constants and the exponents corresponding to the reaction orders were estimated by fitting the model to experimental information.

## 3. Experimental data

In order to validate the proposed model, experimental data obtained in our laboratory were used [7,11,12]. Two groups of experiments may be distinguished: the graft reaction experiments [7,11] and the PS secondary reactions experiments [7,11,12]. The reaction conditions used in both groups are shown in Tables 3 and 4. As already mentioned, PE does not suffer any side reactions under the conditions used to produce the grafting reaction [7].

### 3.1. Graft reaction experiments

The data for the PE-g-PS graft reaction correspond to two different linear low density PE resins, each treated under different reaction conditions as shown in Table 3.

The experimental information on the PE-g-PS synthesis consisted in the mass percent of grafted PS [7,11] and the average molecular weight of unreacted PS measured by Size Exclusion Chromatography (SEC) [11]. The mass of grafted PS was calculated as the difference between the mass of PS in the starting blend (20% w/w) and the mass of unreacted PS remaining in the insoluble fraction after a high-pressure/high-temperature solvent extraction [7,11].
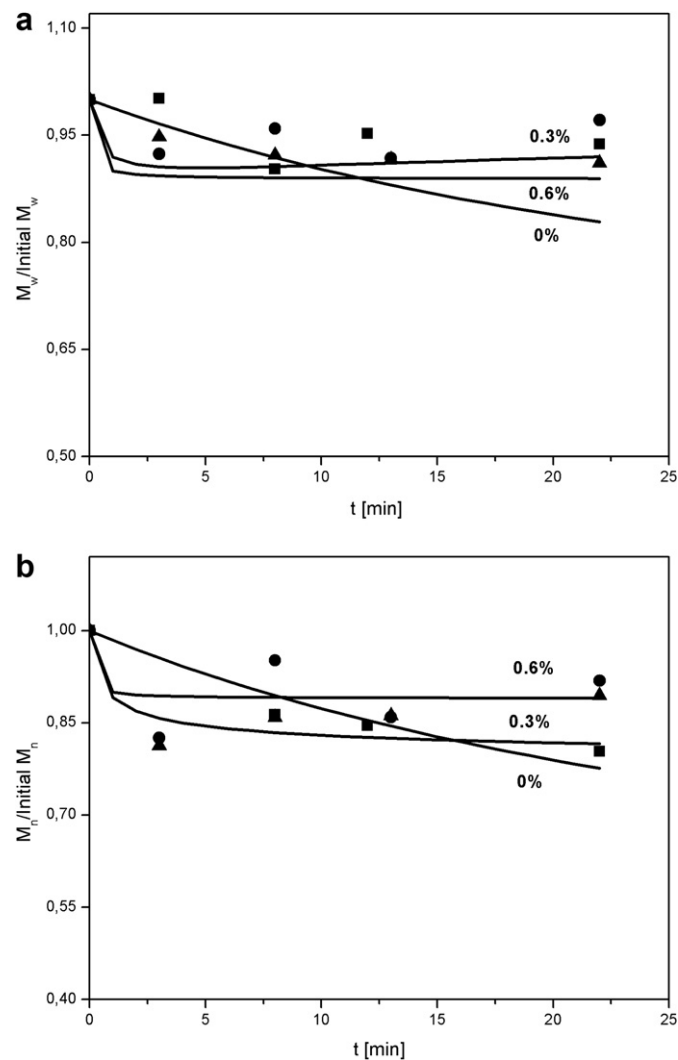
### 3.2. PS side reactions experiments

Data were obtained at two different reaction temperatures. The reaction conditions are shown in Table 4.

**Table 4**
Conditions used for the PS side reactions experiments.

| | | |
|---|---|---|
| Virgin PS | PS ($M_w = 271,000$, $M_n = 136,000$) | |
| Reaction time | 22 min | 10 min |
| Sample withdrawal times | Intermediate and final times | Final time only |
| Initial styrene concentration | 0.0 % wt 0.3 % wt 0.6 % wt | 0.3 % wt |
| Initial AlCl$_3$ concentration | 0.1 % wt 0.3 % wt 0.5 % wt 0.7 % wt 1.0 % wt | 0.1 % wt 0.3 % wt 0.5 % wt 0.7 % wt 1.0 % wt 1.5 % wt |
| Reaction conditions | Batch mixer at 200 °C under N$_2$ atmosphere [12] | Batch mixer at 190 °C under N$_2$ atmosphere [7,11] |

The data obtained from these experiments consist in the number and weight average molecular weights of unreacted PS measured by SEC [11,12] at different reaction times. Reported data correspond to averages of several replications for each data point, ensuring an error level within the instrument accuracy of ±5%.

## 4. Parameter estimation

In this work, kinetic rate constants corresponding to the reactions of PS with AlCl$_3$ and styrene as well as those for the grafting reaction are estimated using the commercial software gPROMS (generalized PROcess Modelling System) and the available experimental data described previously. Preliminary parametric analyses were performed in order to determine the range of parameter values for which each reaction became relevant.

A sequential strategy is used to estimate the kinetic parameters of all the reactions that take place when AlCl$_3$ and styrene are added to a PS/PE blend. To start, the orders of the reactions that involve only PS and AlCl$_3$ were kept equal to those estimated in a previous work [13], that is, for reactions corresponding to Equations (3), (5), (7) and (8) in Table 1. The values for the kinetic rate constants associated to all the side reactions and the deactivation of the catalyst, together with the orders of the reactions that involve styrene were found by fitting the model results to experimental data obtained without PE. These data correspond to reactions of PS with AlCl$_3$ alone [12] and with the system AlCl$_3$/styrene [7,11,12]. In this work the grafting reaction parameters were estimated similarly, using experimental data on



**Fig. 1.** $M_w$ (a) and $M_n$ (b) of PS vs. time. PS treated with 0.1 % wt of AlCl$_3$ and various concentrations of styrene at 200 °C. Lines: model, symbols: experimental measurements [12] (● 0, ■ 0.3, ▲ 0.6% wt styrene).
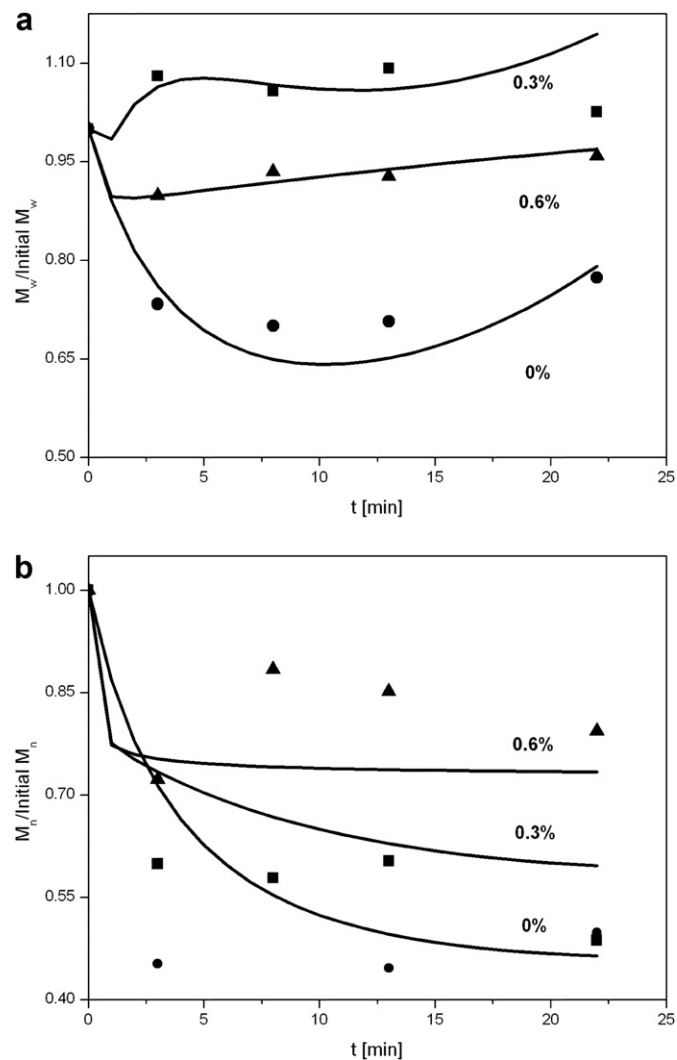
**Fig. 2.** $M_w$ (a) and $M_n$ (b) of PS vs. time. PS treated with 0.3 % wt of AlCl$_3$ and various concentrations of styrene at 200 °C. Lines: model, symbols: experimental measurements [12] (● 0, ■ 0.3, ▲ 0.6% wt styrene).

PS/PE/AlCl$_3$/S [11]. In this system, the PS degradation reactions are less noticeable than in the reaction systems without PE. In order to take this behavior into account in a simple way, we introduced an adjustable factor $ef_2$ that affects all the PS degradation reaction rates. This factor has a value of unity in the absence of PE. This approach avoids the reestimation of a large number of constants.

Since most experiments on the PS secondary reactions were performed at 200 °C, the kinetic rate constants were estimated for this particular temperature. However, the experiments corresponding to the grafting reaction were carried out at 190 °C. If we wanted to account for the effect of temperature by using the Arrhenius expression, $k_j = A_j e^{-E_j/RT}$, we would need to estimate all the $A_j$ and $E_j$, where the subscript $j$ identifies one of the kinetic rate constants of the proposed mechanism. This was not possible because the number of available measurements at different temperatures is insufficient to estimate that many parameters. In order to overcome this problem, we multiplied all kinetic rate constants corresponding to the side reactions by an efficiency factor, $ef_1$, to account for the effect of temperature. The value of this factor was estimated using data from the PS degradation experiments performed at 200 and 190 °C [7,11,12].

The parameter estimation was performed using the commercial software gPROMS, using a weighted least squares approach already described in a previous work [13] that involves both experimental and calculated values. Although in a multiparametric optimization problem such as this one we cannot guarantee to have found the global optimum, the set of kinetic parameters found allow a good representation of the experimental data, as shown below.
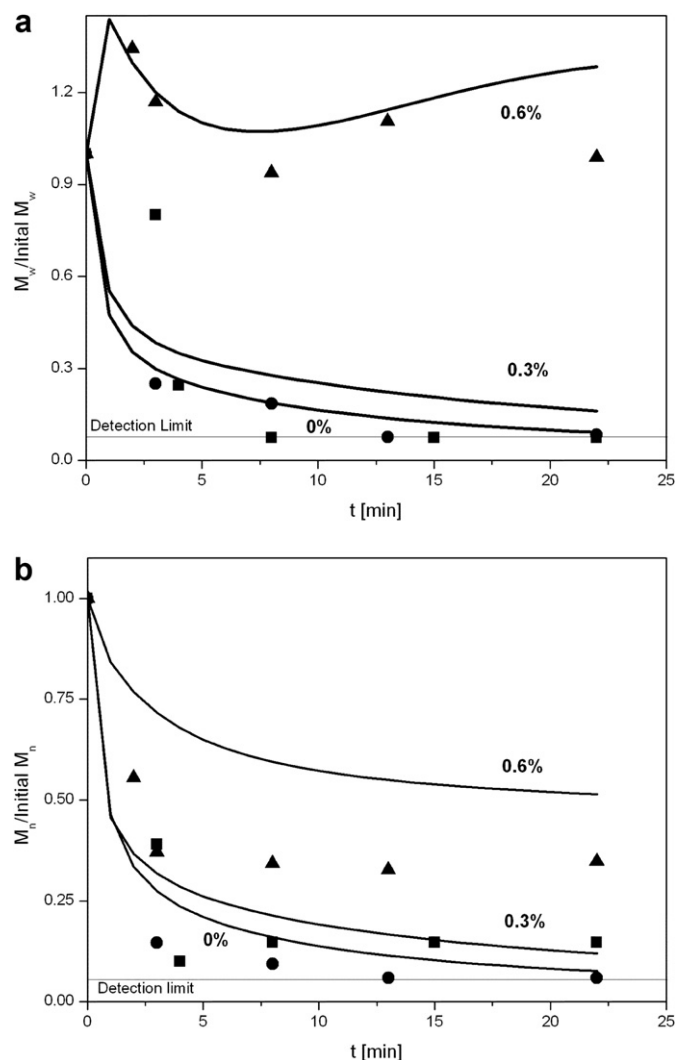
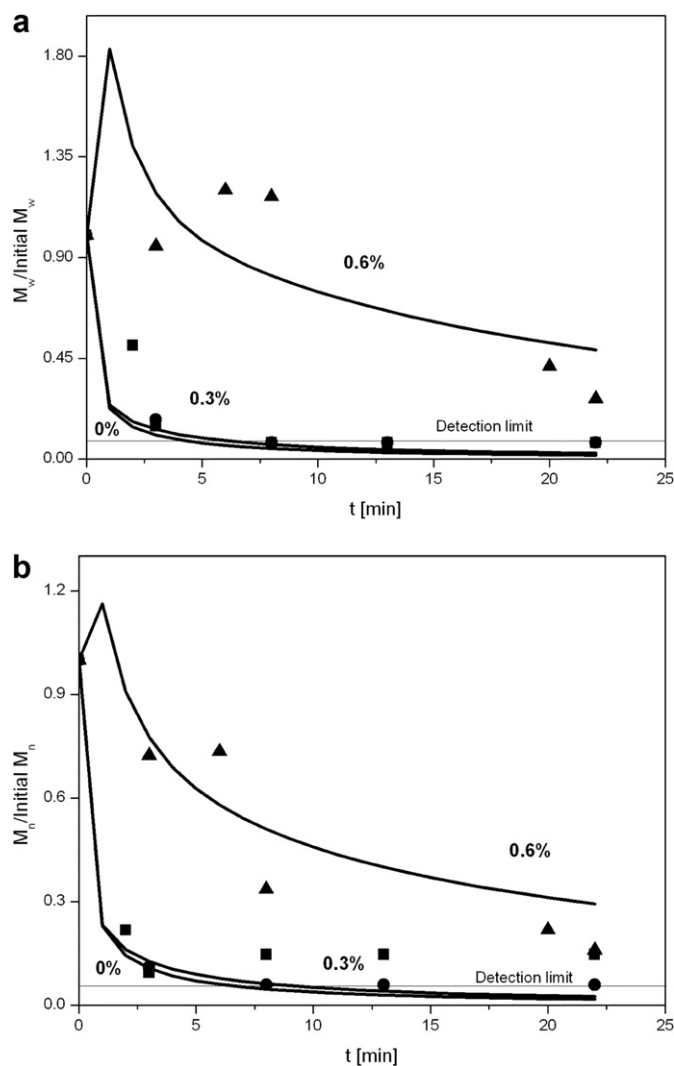## 5. Results and discussion

### 5.1. PS secondary reactions

The catalyst-cocatalyst effect on PS degradation is shown in Figs. 1–5, where the variation of PS average molecular weights is plotted against reaction time for different catalyst and cocatalyst concentrations. In this set of experiments only PS was treated with the catalytic system. As shown, the experimental PS molecular weight exhibits a complex behavior that depends on the ratio between the catalyst ($A$) and cocatalyst ($S$) concentrations. When styrene is absent from the system, PS suffers the greatest degradation levels. If $S/A$ is lower or higher than unity polymer degradation
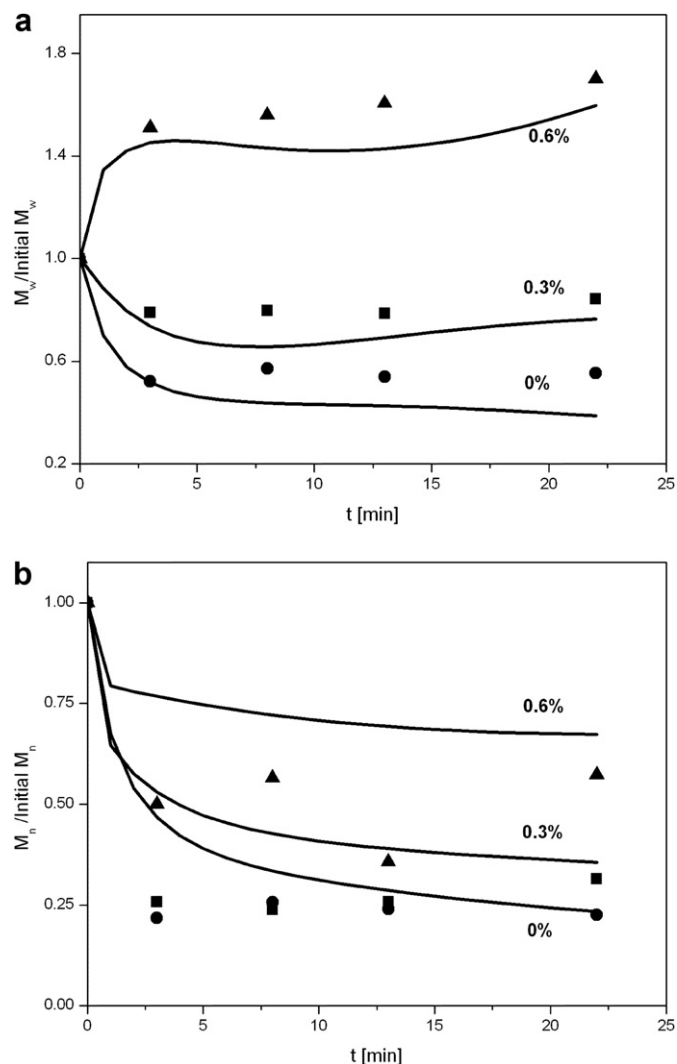


**Fig. 3.** $M_w$ (a) and $M_n$ (b) of PS vs. time. PS treated with 0.5 % wt of AlCl$_3$ and various concentrations of styrene at 200 °C. Lines: model, symbols: experimental measurements [12] (● 0, ■ 0.3, ▲ 0.6% wt styrene).



**Fig. 4.** $M_w$ (a) and $M_n$ (b) of PS vs. time. PS treated with 0.7 % wt of AlCl$_3$ and various concentrations of styrene at 200 °C. Lines: model, symbols: experimental measurements, Ref. [12] (● 0, ■ 0.3, ▲ 0.6% wt styrene).

**Fig. 5.** $M_w$ (a) and $M_n$ (b) of PS vs. time. PS treated with 1.0 % wt of $AlCl_3$ and various concentrations of styrene at 200 °C. Lines: model, symbols: experimental measurements [12] (● 0, ■ 0.3, ▲ 0.6% wt styrene).

**Table 5**
Parameters estimated from the side reaction experiments.

| Parameter | Value |
| --- | --- |
| $k_{S1w}$ | $2.522 \times 10^2 \, M^{-2} \, min^{-1}$ |
| $k_{S1n}$ | $7.149 \times 10^1 \, M^{-4} \, min^{-1}$ |
| $k_{In}$ | $2.000 \times 10^0 \, M^{-2} \, min^{-1}$ |
| $k_{c1}$ | $1.031 \times 10^{-2} \, M^{-3} \, min^{-1}$ |
| $k_i$ | $1.000 \times 10^{-3} \, min^{-1}$ |
| $k_{S2w}$ | $9.260 \times 10^6 \, M^{-5} \, min^{-1}$ |
| $k_{S2n}$ | $4.067 \times 10^4 \, M^{-4} \, min^{-1}$ |
| $k_{c2,1}$ | $8.544 \, M^{-4} \, min^{-1}$ |
| $k_{c2,2}$ | $9.266 \times 10^8 \, M^{-9} \, min^{-1}$ |
| $k_p$ | $7.158 \times 10^7 \, M^{-4} \, min^{-1}$ |
| $k_d$ | $1.329 \times 10^7 \, M^{-4} \, min^{-1}$ |
| $\phi, \kappa, \xi, \omega, \tau, \sigma$ | 2 |
| $\eta, \rho, \upsilon$ | 4 |
| $\lambda, \psi$ | 1 |
| $\chi$ | 3 |

observed. This is a consequence of the highly nonlinear nature of the process.

Figs. 1–5 also show model predictions for these experiments. As can be seen, the model is capable of describing the complex behavior of PS for different combinations of $AlCl_3$ concentrations and $S/A$ ratios. Model predictions indicate that chain combination increases when the $S/A$ ratio is near unity, as shown in Figs. 2a and 3a for PS treated with $S/A = 0.3/0.3$ and $S/A = 0.6/0.5$. Similarly, model results properly predict that chain scission is incremented when the $S/A$ ratio differs from unity, as presented in Figs. 2a and 3a for PS treated with $S/A = 0.6/0.3$ and $S/A = 0.3/0.5$, respectively.

Fig. 1 shows the results for PS treated with the lowest $AlCl_3$ concentration. As may be seen, the model predicts that molecular weight variation is less than 20% for the three styrene concentrations used, a variation consistent with the one measured experimentally.

When high catalyst concentrations are used, 0.7% and 1% wt of $AlCl_3$, (Figs. 4 and 5), model predictions agree well with experimental data, showing that adding 0.3% wt of styrene is not enough to counteract the strong tendency to chain scission caused by $AlCl_3$. Adding styrene curbs the intensity of the scission reaction: as the concentration of styrene increases, molecular weight diminishes less significantly or even increases slightly. This may indicate that for these reaction conditions there is a strong competition between chain scission and chain combination reactions.

In the majority of the cases studied, the prediction of $M_w$ is more accurate than that of $M_n$. This is expected to happen, since $M_w$ is more sensitive to the reaction conditions and has more influence on the parameter estimation results.

### 5.2. PE-g-PS grafting reaction

The estimated parameters for the grafting reaction are shown in Table 6. There, we report the two copolymerization rate constants (see Equations (1) and (2)) together with the factors $ef_1$, and $ef_2$ introduced above and determined using independent data sets. Both $ef_1$, and $ef_2$ multiply the values of the constants $k_{S1w}$, $k_{S1n}$, $k_{In}$, $k_{c1}$, $k_{S2w}$, $k_{S2n}$, $k_{c2,1}$, $k_{c2,2}$, and $k_p$ reported in Table 5. The remaining parameters where kept at the values reported in Table 2.

**Table 6**
Estimated parameters. PE-g-PS grafting reaction.

| Parameter | Value |
| --- | --- |
| $k_{gB}$ (copolymerization) | $6.263 \times 10^{10} \, M^{-3} \, min^{-1}$ |
| $k_{gS}$ (copolymerization) | $1.553 \times 10^9 \, M^{-3} \, min^{-1}$ |
| $ef_1$ | $1.366 \times 10^{-1}$ |
| $ef_2$ | $1.237 \times 10^{-1}$ |

is partially inhibited, as may be observed in the $M_w$ results in Figs. 2a and 3a. In the same figures it is shown that when $S/A$ approaches unity, PS molecular weight tends to grow. This may be explained by the competition between scission and chain combination reactions, which could be expected to have different sensitivities to each component of the catalytic system.

For the present model, the estimated parameters concerning the reactions involving PS, $AlCl_3$ and styrene are shown in Table 5.

In order to estimate the relative importance of the different kinetic constants, we performed a sensitivity analysis for the particular system containing 0.3% each of $AlCl_3$ and $S$. The value of each kinetic constant was varied by ±20%, keeping the rest at their optimal values. The effect of this change on the prediction of $M_w/M_{w0}$ and the percentage of grafted PS was evaluated. We found that changing the kinetic constants by 20% induces changes in $M_w/M_{w0}$ of at most 15%. The chain combination constants $k_{c1}$ and $k_{c2,1}$ induce the largest changes. The styrene polymerization constant $k_p$ and the scission of weak links $k_{S1w}$ induce intermediate changes of up to 10%. The remaining constants induce changes smaller than 5%. The percentage of grafted PS was essentially insensitive to this one-by-one kinetic rate constant change. If, however, all kinetic constants changed simultaneously by 20%, differences of up to 25% could be
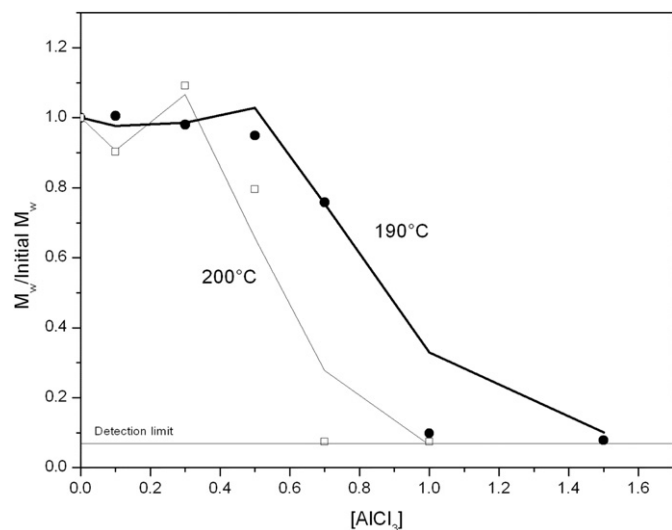
**Fig. 6.** Final $M_w$ vs. [AlCl$_3$] for PS treated with 0.3% wt of styrene. Lines: model, symbols: experimental measurements [7,11,12] ( ● 190 °C, □ 200 °C).



**Fig. 8.** Evolution of the final $M_w$ of unreacted PS with [AlCl$_3$], treated with 0.3% wt of styrene at 190 °C. Lines: model, symbols: experimental measurements [11].

It is important to note that, as already stated, most of the PS side reaction measurements were performed at 200 °C, while those of the grafting reaction were performed at 190 °C. The efficiency factor, $ef_1$, was estimated in order to take the effect of temperature into account. For this task, we used data from the PS degradation experiments performed at 190 °C [7,11].

The results of PS degradation performed at 190 °C are shown in Fig. 6, where $M_w$ is plotted as a function of the concentration of AlCl$_3$. The pronounced effect of temperature on PS degradation may be seen when comparing these results with those obtained at 200 °C. This effect is properly described by the model predictions. The estimated value for $ef_1$ (see Table 6) indicates that lowering temperature by 10 °C causes the kinetic rates of side reactions to drop by 87%. Moreover, these predictions are in agreement with the data reported by Guo et al. [9] and Gao et al. [10], who studied the PS/PO reactive compatibilization. They reported that for experiments performed at temperatures under 180 °C, PS was not degraded even when high AlCl$_3$ concentrations were used.

Finally, we studied the grafting reaction for the two PE resins used in this work. The progress of the reaction was evaluated by
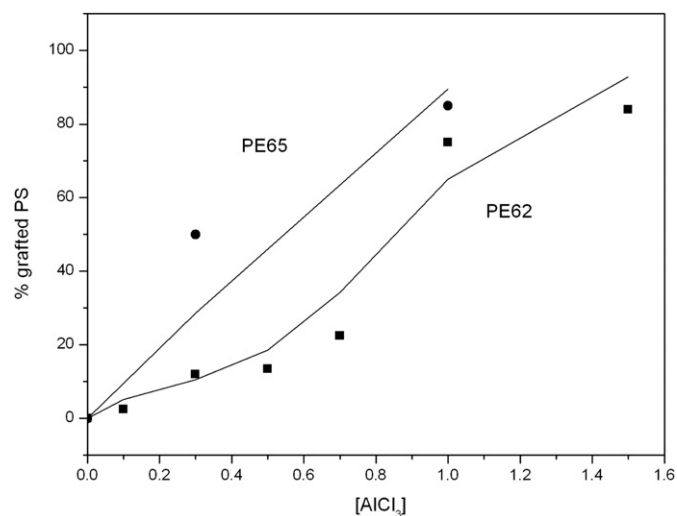


**Fig. 7.** Final grafted PS [% wt] vs. [AlCl$_3$] for 0.3 % wt of styrene and two PE resins at 190 °C. Lines: model, symbols: experimental measurements [7,11] ( ● PE62, ■ PE65).
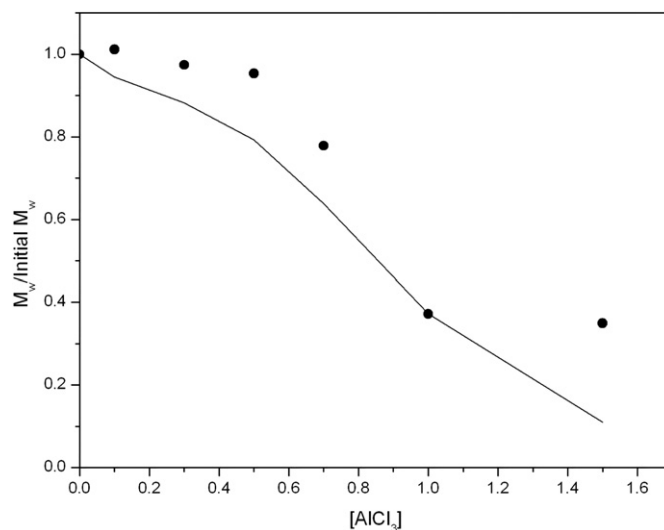
analyzing the reported experimental data on the mass of grafted PS for different catalyst concentrations [7,11]. As shown in Fig. 7, the mass of grafted PS increases with catalyst concentration. The data suggest that the molecular weight of PE also influences the amount of grafted PS. For these experiments, the mass of grafted PS was highest when using the PE of lowest molecular weight. As already reported [3,7,23,24], short molecules are expected to be more reactive because they are more likely to be situated at the PE/PS interface. In our model this effect is taken into account by the reactivity factor, $f_r$, that reduces the grafting reactivity of the larger molecules. On the other hand, the influence of the catalyst may be explained not only by its direct participation in the copolymerization reaction but also by the generation of shorter, more reactive PS chains through the scission reaction.

Fig. 7 also shows the calculated mass of grafted PS. As shown, both the effect of PE molecular weight and AlCl$_3$ concentration are properly described by the model.

As an example of the capabilities of the model, we show in Fig. 8 the measured $M_w$ of the unreacted PS for the grafting experiments conducted with PE62, together with the model predictions. Although the model is capable of describing the general trend, indicating that $M_w$ in the unreacted PS diminishes as the concentration of AlCl$_3$ increases, the calculated values are consistently lower than the experimental measurements. This systematic error may be due to the limitations of the method used to separate the unreacted PS from the copolymer and the unreacted PS, a high-pressure/high-temperature extraction procedure [7]. Martini et al. [27] reported that at the same extraction conditions and at high catalyst concentrations, PS degradation was so important that some of it remained with the copolymer, leaving only the higher molecular weight PS molecules available for analysis.

## 6. Conclusions

A model for the graft copolymerization of PS and PE in the presence of AlCl$_3$ and styrene was developed. The model included some PS side reactions that influence the amount of copolymer formed and its composition. Kinetic parameters, such as kinetic rate constants and reaction orders, were estimated with the aid of published experimental data. The model agreed well with experimental data such as average molecular weights and mass of grafted PS. It is also able to describe the influence of catalyst concentration and PE chain length.

In order to select operating conditions appropriate for a compatibilization application, several aspects should be taken into account. As already mentioned, shorter homopolymer molecules increase the amount of copolymer formed, but compatibilization has been found to be more effective when the copolymer contains long homopolymer blocks [7]. Thus, these competing effects must be considered when selecting optimal operating conditions. Other variables that play an important role are the catalyst and cocatalyst concentrations. Since experimental determination of the optimal conditions is a difficult task, the mathematical model presented in this work seems to be a useful tool to select them. Work is under way in this direction.

## Acknowledgments

## References

[1] Bisio AL, Xanthos M. How to manage plastics waste: technology and market opportunities. Munich: Hanser; 1995.
[2] Barentsen WM, Heikens D. Polymer 1973;14(11):579–83.
[3] O'Shaughnessy B, Sawhney U. Macromolecules 1996;29(22):7230–9.
[4] Sundararaj U, Macosko CW. Macromolecules 1995;28(8):2647–57.
[5] Carrick WL. J Polym Sci A Polym Chem 1970;8(1):215–23.
[6] Sun YJ, Baker WE. J Appl Polym Sci 1997;65(7):1385–93.
[7] Díaz MF, Barbosa SE, Capiati NJ. Polymer 2007;48(4):1058–65.
[8] Díaz MF, Barbosa SE, Capiati NJ. Polymer 2002;43(18):4851–8.
[9] Guo Z, Fang Z, Tong L, Xu Z. Polym Degrad Stabil 2007;92(4):545–51.
[10] Gao Y, Huang H, Yao Z, Shi D, Ke Z, Yin J. J Polym Sci B Polym Phys 2003;41 (15):1837–49.
[11] Díaz MF, Barbosa SE, Capiati NJ. In: Kyu T, Nwabunma D, editors. Polyolefin blends. New York: Wiley & Sons; 2007 [chapter 20].
[12] Díaz MF, Barbosa SE, Capiati NJ. J Appl Polym Sci 2009;114(5):3081–6.
[13] Gianoglio Pantano IA, Díaz MF, Brandolin A, Sarmoria C. Polym Degrad Stabil 2009;94(4):566–74.
[14] Nanbu H, Sakuma Y, Ishihara Y, Takesue T, Ikemura T. Polym Degrad Stabil 1987;19(1):61–76.
[15] Chiantore O, Camino G, Costa L, Grassie N. Polym Degrad Stabil 1981;3(3): 209–19.
[16] Rabek JF, Lucki J. J Polym Sci A Polym Chem 1988;26(9):2537–51.
[17] Tarakeshwar P, Kim KS. J Phys Chem A 1999;103(45):9116–24.
[18] Gugumus F. Polym Degrad Stabil 2006;91(6):1333–45.
[19] de Kock RJ, Hol PAHM. J Polym Sci B Polym Lett 1964;2(4):339–41.
[20] Miskolczi N, Bartha L, Deák G, Jóver B, Kalló D. J Anal Appl Pyrol 2004;72(2): 235–42.
[21] Aguado J, Sotelo JL, Serrano DP, Calles JA, Escola JM. Energ Fuel 1997;11(6): 1225–31.
[22] McCoy BJ, Wang M. Chem Eng Sci 1994;49(22):3773–85.
[23] Broseta D, Fredrickson GH, Helfand E, Liebler L. Macromolecules 1990;23(1): 132–9.
[24] Kramer EJ. Isr J Chem 1995;35(1):49–54.
[25] Díaz MF. Doctoral Thesis, Universidad Nacional del Sur; 2004.
[26] Zabisky RCM, Chan W-M, Gloor PE, Hamielec AE. Polymer 1992;33(11): 2243–62.
[27] Martini RE, Barbosa S, Brignole E. Ind Eng Chem Res 2006;45(10):3393–9.